Applied Nanoscience (2021) 11:2459–2467
https://doi.org/10.1007/s13204-021-02073-2

ORIGINAL ARTICLE

Enhanced electrochemical performance of redox conductive polymer in the presence of high efficient modified reduced graphene oxide

Peyman Khodaei kahriz[1] · Ali Ehsani[2] · Ali Akbar Heidari[1] · Hossein Mahdavi[1] · Mohammad Bigdeloo[2] · Mehdi Kalhor[3]

Received: 11 June 2021 / Accepted: 28 August 2021 / Published online: 23 September 2021

Abstract

In the present study, we introduce a simple chemical method to synthesize p-phenylenediamine (PPD) as an efficient material for functionalizing graphene oxide. Functionalized reduced graphene oxide Aerogel with PPD (PPD-rGO Aerogel) is used for improving electrochemical performance of polyorthoaminophenol electroactive film. The structural morphology and microstructure analysis of the materials used in this work are performed by different surface analyses. The composite electrode's electrochemical behavior is studied using an acidic solution in cyclic voltammetry (CV) and charge/discharge system. The POAP/PPD-rGO composite electrode shows a C_s of 1180 F/g at 1.0 A/g current density. Our results provide an improved conductive polymer composite film with high active surface area, ease of synthesis and high cycling stability for supercapacitors (SCs).

Keywords rGO · Aerogel · Supercapacitor · Impedance

Introduction

Because of the rapidly growing demand for green energy, the researchers' efforts are focused on the exploration of efficient, clean and sustainable equipment for energy storage (Ehsani et al. 2021a). Supercapacitors are known for their exceptional energy storage with rapid charge/discharge, long cycle-life, and wide temperature range (Burke 2000). Therefore, SCs are considered one of the promising electrical energy storage devices that might replace the present battery technology for efficient energy storage applications in portable and wearable electronics, and electric and hybrid vehicles (Kaempgen et al. 2009; Zhao et al. 2012; Hu et al. 2011). Different materials such as CNT, graphene (Kong et al. 2018; Chen and Xue 2014, 2015, 2017; Kang et al. 2017; Chen et al. 2015a, b, 2017; Liu and Xue 2013, 2015; Liu et al. 2012) and activated carbon (Chen et al. 2011; Yu et al. 2009) have been studied as active materials in double layer capacitor due to their significantly high surface area. However, it has been reported that conducting polymer (CP) and transition metal oxide (TMO)-based electrode materials show pseudo-capacitance behavior (Shakir et al. 2020). Polyaniline (PA) and poly orthoaminophenol (POAP), among pseudo-capacitive polymers, are being significantly investigated due to their features such as flexibility, ease of synthesis, high energy density and great power density (Eftekhari et al. 2017; Mohilner et al. 1962; Moussa et al. 2016).

However, durable electrochemical performance of POAP still suffers serious losses due to its low conductivity and decomposing during the consecutive charge process. Many studies have been done on the constructing of different composite to improve the cyclic stability of POAP, which could easily accommodate their volume change (Meng et al. 2013a; Ehsani et al. 2019a). Investigation of graphene composite has attracted growing interest in the field of electrochemical capacitors and batteries (Meng et al. 2013b). Accordingly, we designed and prepared POAP/PPD-rGO composite with an ideal structure by electrochemical technique. These results demonstrate that the POAP/PPD-rGO

✉ Ali Ehsani
ehsani46847@yahoo.com; a.ehsani@qom.ac.ir

✉ Hossein Mahdavi
hmahdavi@khayam.ut.ac.ir

[1] School of Chemistry, College of Science, University of Tehran, P.O. Box 14155–6455, Tehran, Iran

[2] Department of Chemistry, Faculty of Science, University of Qom, Qom, Iran

[3] Department of Organic Chemistry, Payame Noor University, 19395-4697 Tehran, Iran

composite with the desirable electrochemical features can be a promising active compound for the development of SCs.

Experimental

Characterization

The instrument used in the electrochemical performance test process is Ivium V21508, Vertex electrochemical analyzer. In the three-electrode system, carbon paste, a platinum plate, and Hg/HgO electrodes were employed as the working electrode, counter electrode, and the reference electrode, respectively. We used 1.0 M $HClO_4$ as the acidic electrolyte. The electrochemical behaviors are characterized and tested by cyclic voltammetry and constant-current galvanostatic. The charge transfer mechanism in electrochemical process is further investigated by electrochemical impedance spectroscopy (EIS) over the frequencies of 0.01–100,000 Hz with 5 mV amplitude at the open circuit potential condition. The morphology of polymeric films was investigated by SEM analysis. Morphology and particle dispersion were studied by scanning electron microscopy (SEM) (Cam scan MV2300). X-ray diffraction (XRD) patterns were obtained from an X-ray diffractometer (PANalytical X'Pert-Pro) with a Fe–K^{α} monochromatized radiation source.

Synthesis of PPD-rGO aerogel

The schematic description of the method applied for the synthesis of PPD-rGO is exhibited in Scheme 1. Accordingly, the reduction of GO was carried out using PPD as an suitable reducing substance through the facial hydrothermal approach, leading to the formation of PPD-rGO aerogels, in which PPD molecules are capable of providing more free spaces between graphene sheets arising from the reaction between $–NH_2$ functional groups of PPD and oxygen ones providing by GO sheets. Finally, a freeze dryer instrument was employed to dry the as-prepared materials and fabricate the final solid product.

Synthesis of poly orthoaminophenol and poly orthoaminophenol/PPD-rGO

Poly orthoaminophenol/PPD-rGO composites were prepared by in a stirring solution containing 0.01 M monomer (ortho aminophenol), 1.0 M perchloric acid, 0.1 M lithium perchlorate and 5.0×10^{-3} M SDS on the surface of the PPD-rGO aerogel modified WE. Poly ortho aminophenol electrode was synthesized in same solution without PPD-rGO in the surface of the carbon electrode. Forty consecutive cycles was used for electropolymerization of polymer and composite on the surface of the working electrode (Sadeghinia et al. 2019; Ehsani et al. 2018a, 2021b; Kahriz et al. 2020).

Results and discussion

The FTIR spectra of GO and PPD-reduced graphene oxide are depicted in Fig. 1A, through which the changes in the functional groups can be easily demonstrated. After the oxidation of graphite, the characteristic bands corresponding to epoxy C–O, C=C, C=O (carbonyl and carboxylic acid moieties), and O–H stretches emerged at 1052, 1630, 1741, and 3420 cm^{-1}, demonstrating the successful oxidation reaction (Zhang et al. 2013). In addition, after the reduction reaction, it was observed that the peaks at 1741 and 1052 cm^{-1} disappeared in the spectrum of PPD-rGO and new bands emerged

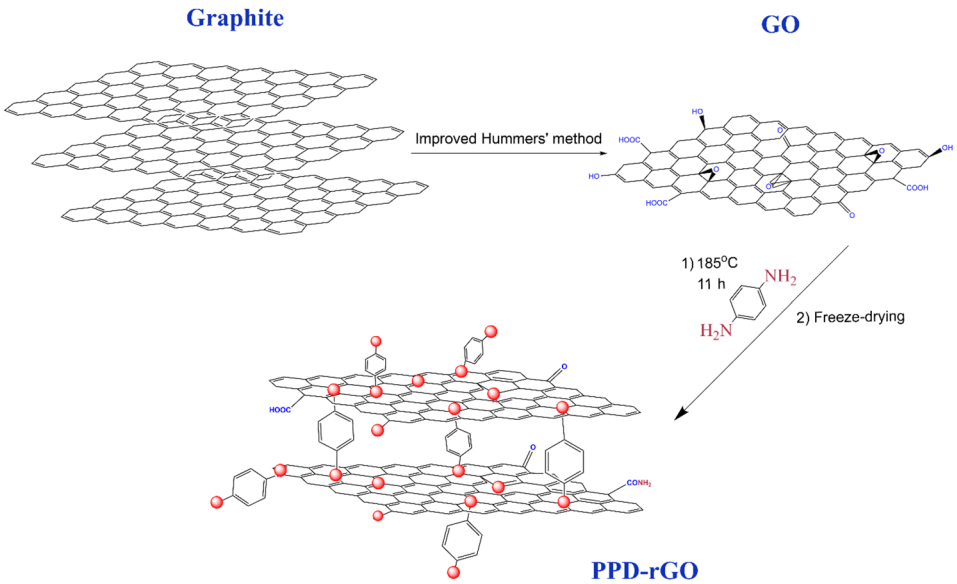

Scheme 1 Schematic representation of the procedure used for the fabrication of PPD-rGO

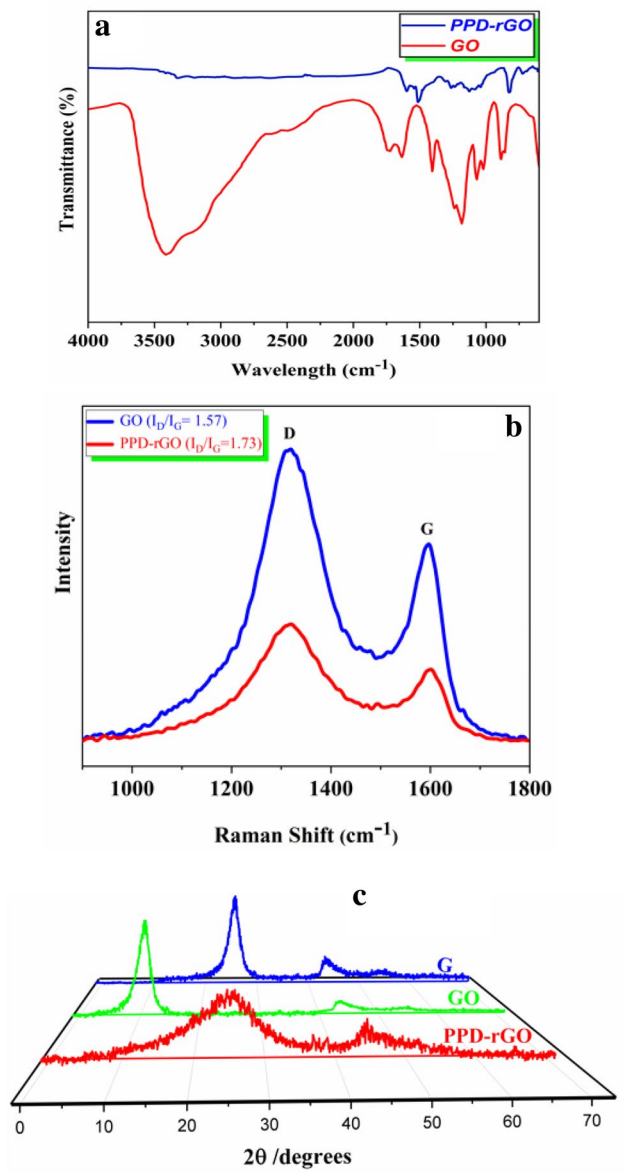

Fig. 1 **A** The FTIR spectra corresponding to GO (the red line) and PPD-rGO (the blue line). **B** Raman spectra of GO (the blue line) and PPD-rGO (the red line) and **C** the XRD peaks corresponding to graphite (the blue line), GO (the green line) and PPD-rGO (the red line)

at 1265 and 1542 cm^{-1} attributing to sp^2 bonded C–N and N–H bend vibrations (Peng et al. 2013). Accordingly, it is demonstrated that the oxygen-containing functional groups existing in GO have reacted with the –NH_2 ones existing in PPD, by which new other covalent bonds have been formed.

Raman spectroscopy analysis was carried out for investigating how the disorder degree of the fabricated PPD-rGO samples is affected by PPD, as the reducing agent. Accordingly, the D band (1366 cm^{-1}) and G band (1576 cm^{-1}) can be easily seen in both spectra shown in Fig. 1B. It is well known that the D band related to the formation of disorder carbon and defects in the graphitic layers involves grain boundaries as well as hetero-atoms embedded in the structure of graphene planes. On the other hand, the G band (the 1st order scattering of E_{2g} vibrational mode in plane) is related to sp^2 hybridized C–C bonds existing in a 2-D hexagonal lattice (Gholipour-Ranjbar et al. 2016). In addition, it is worth pointing out that I_D/I_G have been extensively employed by researchers for the purpose of evaluating the quality of the fabricated carbon materials. It was found that I_D/I_G of the prepared PPD-rGO aerogel (assessed at 1.73) was more than that of GO (assessed at 1.57), which strongly demonstrated the successful modification of GO with doped defects (Mahdavi et al. 2017; Yu et al. 2016).

The results corresponding to structural analyses, conducted by applying an XRD instrument, are presented in Fig. 1C, in which the peaks related to graphene, GO and PPD-rGO samples are exhibited. For GO, the peak at about 10.22° is attributed to (002) plane (Dezfuli et al. 2015), which entirely disappeared after functionalization of GO. Additionally, a weak and broad peak emerged around 24.6° in the spectrum represented by PPD-rGO which is attributed to the (002) plane of G (Bharath et al. 2015). All the provided results demonstrate the fruitful reduction of graphene oxide.

As can be seen in Fig. 2A, the surface chemical composition along with the changes in the functional groups in both GO and the fabricated PPD-reduced graphene oxide was analyzed by using XPS analysis as an efficient method. It is obvious in Fig. 4A, in the XPS spectrum of GO, that two peaks which are attributed to C1s and O1s energy are located at 285.1 and 531.9 eV. Based on the Fig. 4A, the peak appeared at about 400 eV is related to N1s, by which the fruitful reduction of graphene oxide using PPD can be strongly confirmed. Close investigation of the N1s peak, as exhibited in Fig. 4B, indicated presence of pyridinic N, amino N, pyrrolic N and graphitic N. It is worth pointing out that the surface functionalization of GO can be easily confirmed by the amine N1s peak. Moreover, by drawing a comparison between the C1s/O1s intensity ratio in graphene oxide and that of the fabricated PPD-rGO aerogel, a considerable increase in the intensity ratio can be observed, by which the fruitful N-doping is confirmed. XPS data confimed presence of 7.09 at% in the prepared PPD-rGO.

For the purpose of analyzing the morphological architecture of the prepared GO and PPD-rGO aerogel, FESEM analysis was utilized (Fig. 3A, B). Close investigation of the images provided for GO (Fig. 2A) demonstrates that crumpled, wrinkled and folded sheets which are closely attached to each other, as a result of the harsh oxidation process in the Hummer's approach, causing innumerable oxygen-containing functional groups in the structure, have constructed the structure of GO layers (Drmosh et al. 2019). Nonetheless, by drawing a comparison with GO

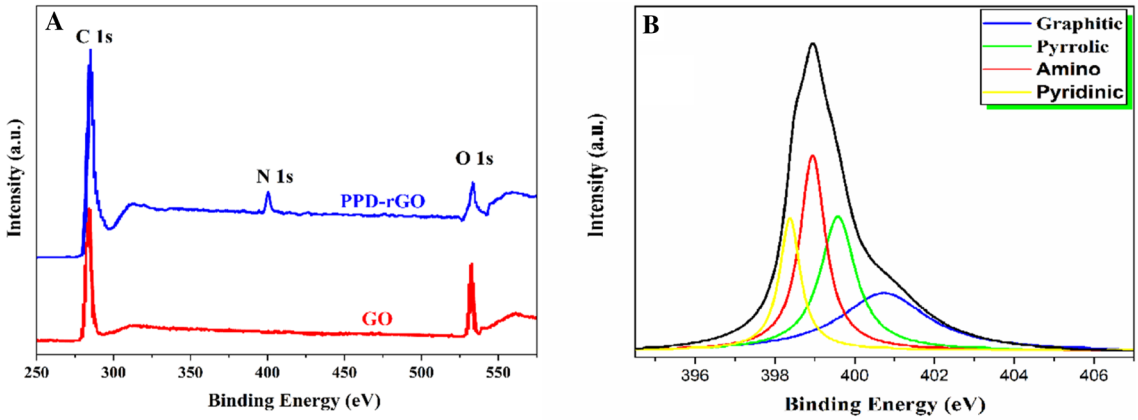

Fig. 2 **A** The XPS data presented by graphene oxide and the fabricated PPD-reduced graphene oxide, and **B** XPS spectra of the N1s

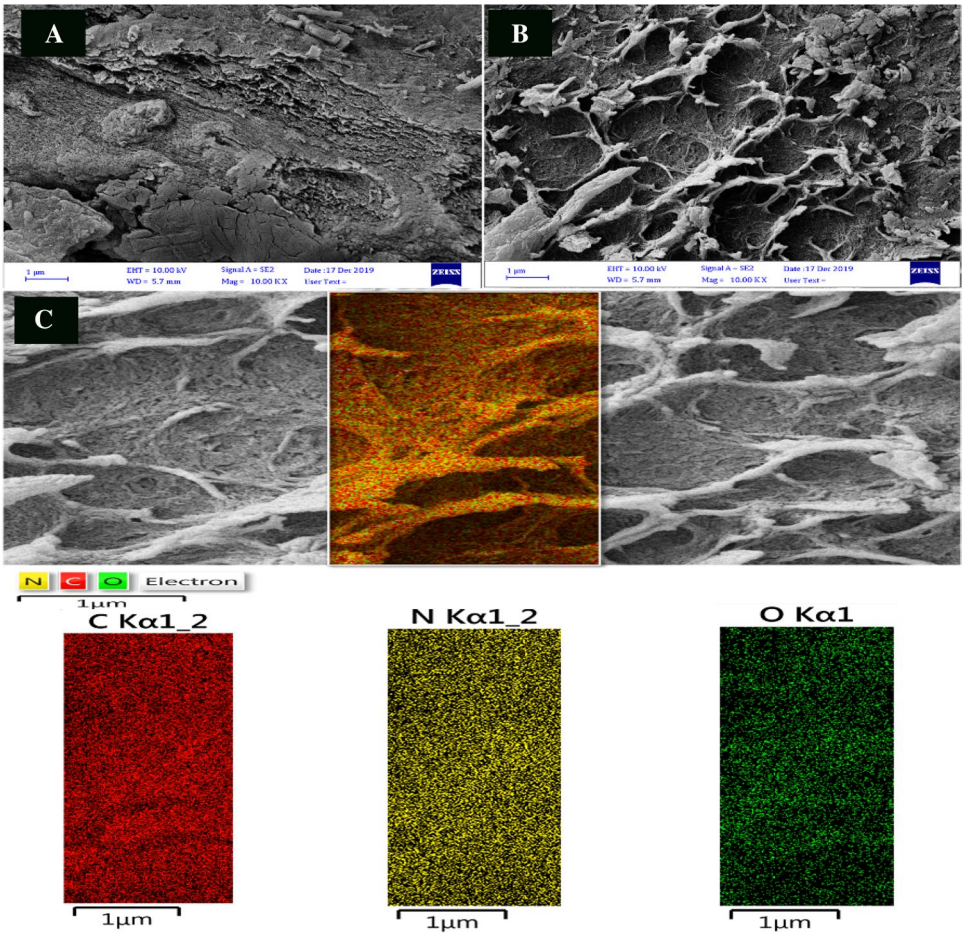

Fig. 3 SEM images of **A** graphene oxide and **B** PPD-reduced graphene oxide and **C** element mapping of PPD- reduced graphene oxide

sheets, it can be indicated that an ultrathin sheet-like morphology with macro pores, a well-defined porous network and much lower agglomerations is provided by the fabricated PPD-rGO aerogel, as exhibited in Fig. 3B, by which the successful reduction of GO through the utilization of PPD is demonstrated.

The distribution along with the atomic and weight percentage of carbon, nitrogen and oxygen in the PPD-rGO aerogel was investigated by using quantitative dispersive X-ray spectroscopy (EDX) element mapping. As can be seen in Fig. 3C, carbon, nitrogen and oxygen atoms are homogeneously distributed on the whole surface of the prepared

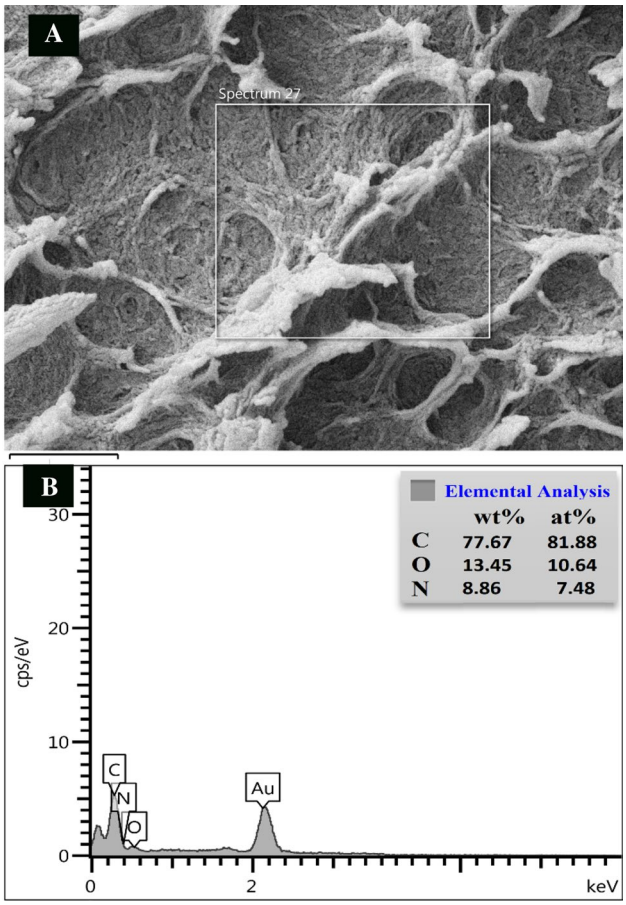

Fig. 4 The EDX spectrum of the fabricated PPD- reduced graphene oxide

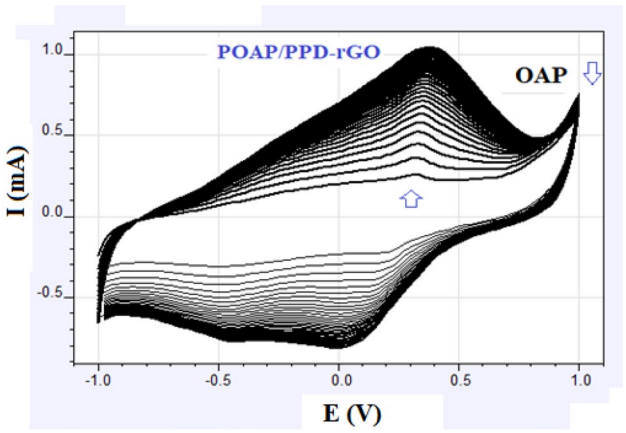

Fig. 5 Consecutive CV for polymerization of POAP in the presence of PPD- reduced graphene oxide

PPD-reduced graphene oxide, observed in the selected area, demonstrating the excellent distribution of PPD as the reducing agent. Moreover, the corresponding EDX data of the fabricated PPD–reduced graphene oxide are represented in Fig. 4, providing a quantitative analysis by which the atomic percentage of C, O and N have been assessed at 81.88 at%, 10.64 at% and 7.48 at%, respectively. It is worth pointing out that, by drawing a comparison with GO (considering the results obtained from XPS analysis as 61.44 at% C and 38.56 at% O), the low oxygen content existing in PPD-rGO aerogel strongly demonstrates the outstanding efficiency of PPD in reduction of GO (Kumar et al. 2018).

Consecutive cyclic voltammograms of electropolymerization of POAP in the presence of PPD- reduced graphene oxide are shown in Fig. 5. Cation radical and oligomer formed from the oxidation of OAP monomer resulted in formation of POAP. Enhanced peak in 0.3 V is related to oxidation of formed conductive polymer. Presence of the PPD- reduced graphene oxide increased polymerization rate via reducing repulsive center during oxidation of monomer.

Figures 6 shows the CV curves of prepared electrodes at specific potentials window and scanning rates. A pair of cathodic/anodic peaks emerged on the CV curves of electrode materials, indicating that they all exhibited pseudocapacitive mechanism for charge storage. At the sweeping rate of 100 mV/s, the CV curves of POAP/PPD-rGO exhibited larger peak areas, indicating that the electrochemical capacitance of POAP/PPD-rGO could have been better than POAP. Moreover, the CV voltammograms of the composite electrode has a slight slope at high potentials, indicating better storage performance and lower resistivity. In addition, improved performance is related to synergistic effect between POAP and PPD-rGO. Also, the reversibility reaction among the composite and electrolyte confirmed by symmetric voltammograms of POAP/PPD-rGO.

The effect of the applied sweep rate on the electrochemical performance of the prepared electrodes is shown in Fig. 6B. An apparent pair of redox peaks still can be distinctly recognized even at the scan rate of 400 mV s^{-1}, suggesting that the POAP/PPD-rGO is beneficial to fast redox reactions. Additionally, low shift for the redox peak potential is observed for increasing scan rates, which can be owning to excellent conductivity of prepared electrode.

Although CV can be used to determine the specific capacitance of the redox materials, the galvanostatic charge/discharge (GCD) curve closely reflects the potential practical use of the electrode material for the supercapacitor device applications for a 2-electrode device system. To know the composite's supercapacitive behavior, GCD was carried out at different current densities (Fig. 7B). The shape of the GCD curves for POAP/PPD-rGO did not appear to be exactly triangular as we observed for pseudo-capacitive material. Instead, it exhibits a non-linear discharge response due to the presence of a faradaic type of material in the

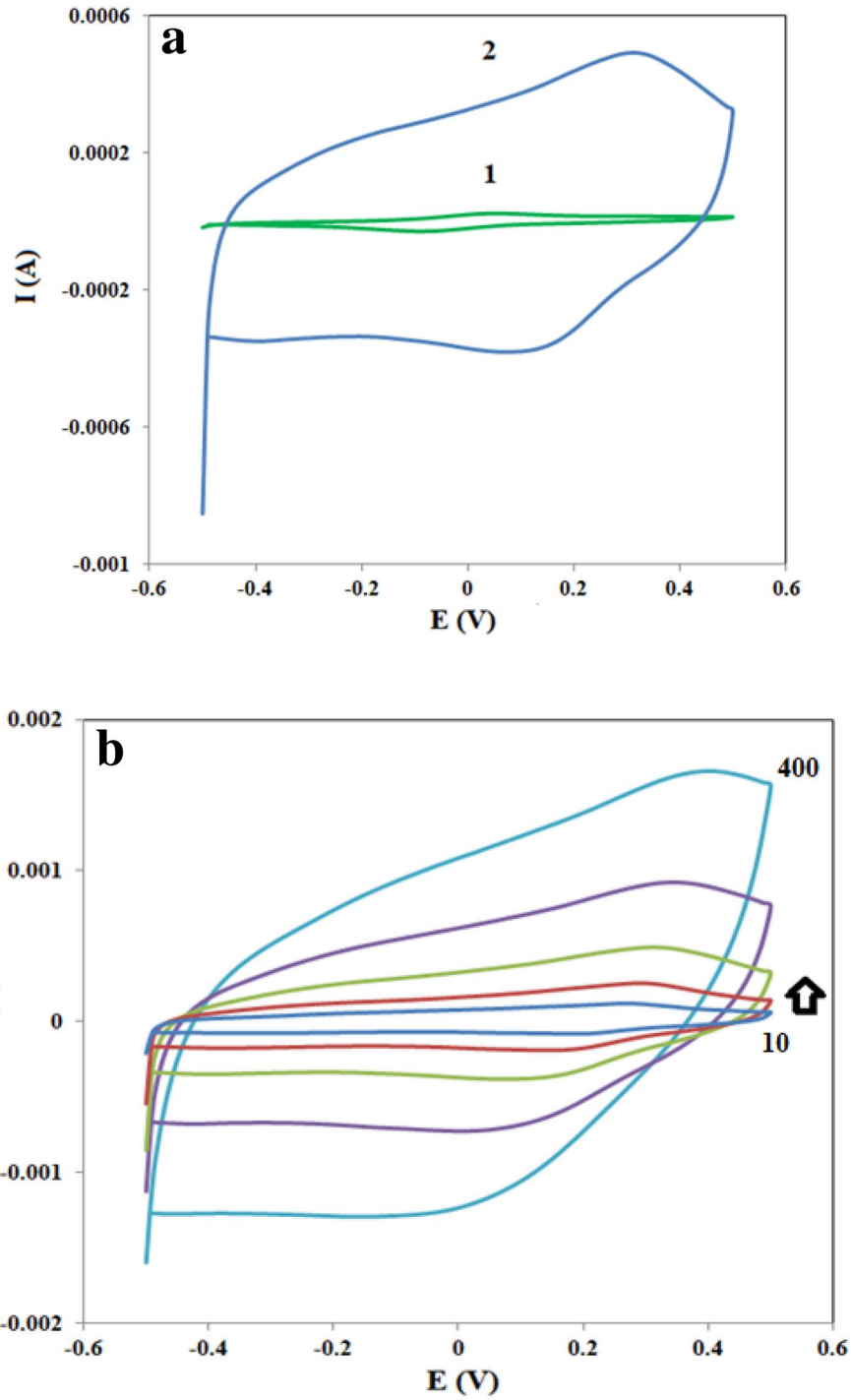

Fig. 6 **A** CV of polymer and prepared graphene composite in 1 M $HClO_4$ and **B** CV of prepared composite electrode in different scan (10-400 mV/s)

nanocomposite, which undergoes redox reactions during charge and discharge of the device.

The Cs of 1180F/g at current density of 1A/g was obtained from the discharge curves (Ehsani et al. 2018b, 2019b, 2020; Shiri et al. 2017a, b, 2018, 2019; Naseri et al. 2016; Sadeghi et al. 2020; Shayeh et al. 2017). Based on the obtained charge/discharge curve in Fig. 7C, D, the POAP/PPD-rGO electrode revealed the highest areal capacitance at high current density. Furthermore, the specific capacitances of POAP/PPD-rGO electrode were also competitive to most of reported POAP based electrode materials (Ehsani et al. 2018a, 2019a, 2020; Shiri et al. 2017a, b, 2018, 2019; Naseri et al. 2016; Sadeghi et al. 2020).

The capacitance retention of composite electrode was studied for consecutive C/D in acidic media at high current density. As shown in Fig. 7C, D, C_s of the polymer

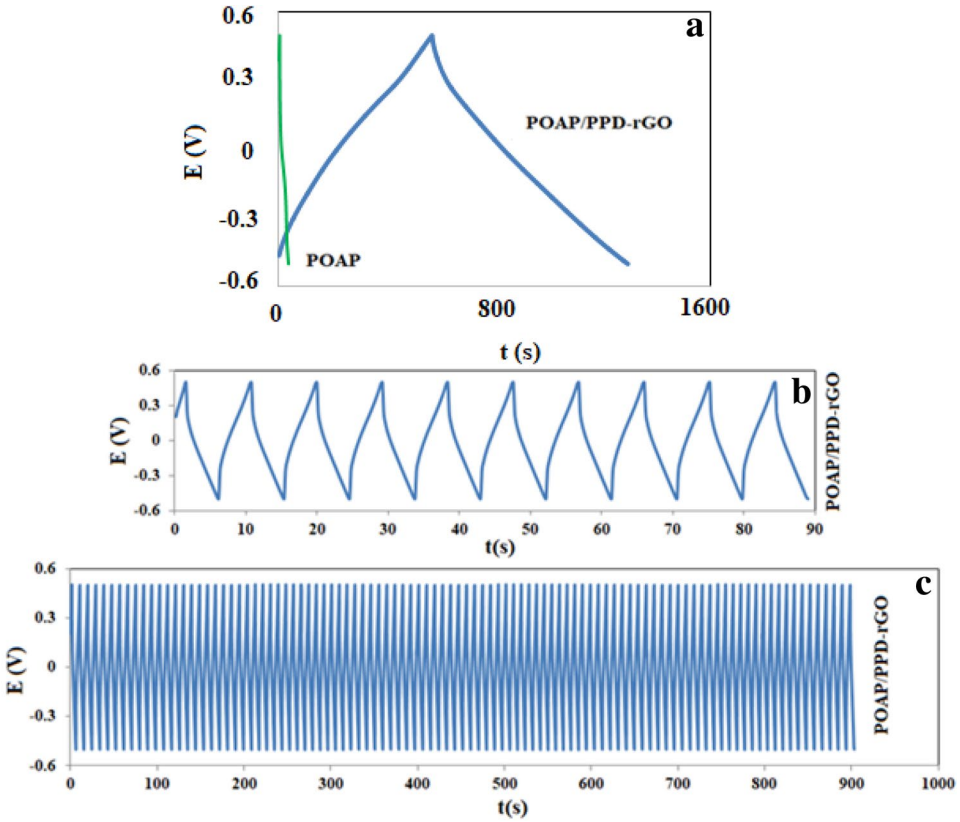

Fig. 7 GCD of **A** polymer and composite electrode at 1 A/g **B** during 10 and **C** 100 consecutive GCD in high current density

film dramatically decreases due to degradation process duding consecutive charge/discharge. Presence of PPD-rGO in POAP/PPD-rGO dramatically modified its capacitance retention, due to synergism effect between POAP/PPD-rGO and pure polymer film. Therefore, the value of 91% was obtained for retention capacitance of prepared composite film during consecutive 3000 cycles.

EIS as a powerful technique was conducted to determine the electrical characteristic parameters of the electrode–electrolyte interface over a wide range of frequencies (Sadeghi et al. 2020; Shiri et al. 2018; Ehsani et al. 2011, 2018b, 2021c, d; Shayeh et al. 2017; Mahjani et al. 2010; Shabani-Shayeh et al. 2015). The EIS data of fabricated samples were employed to draw their Nyquist plots as displayed in Fig. 8. From Nyquist plot, it is evident that it consists of a semicircle indicating high frequency related to charge transfer resistance *R*ct. A straight line in a low-frequency region is related to ions diffusion mechanism. It has been evident that lower value of charge-transfer resistance (*R*ct) results in enhanced conductivity as in the presence of PPD-rGO. Evidently, presented composite electrode showed lower diameter compared to POAP (Mahjani et al. 2010), indicating smaller R_{ct} and higher specific capacitance.

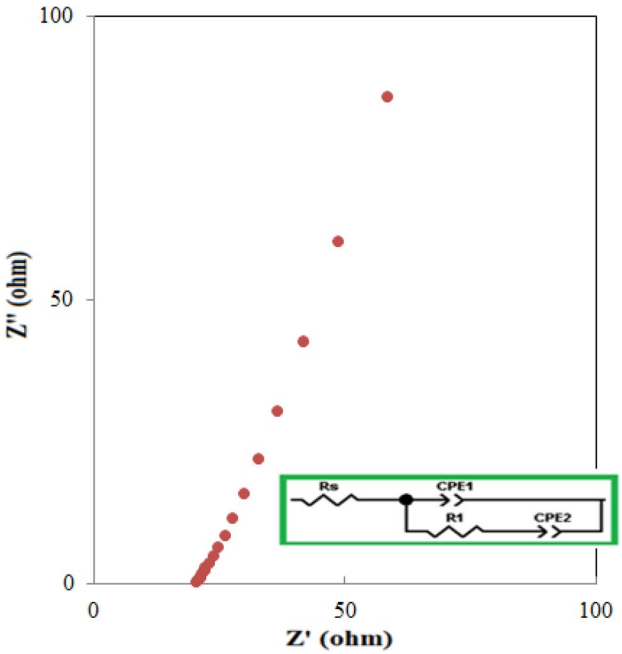

Fig. 8 Nyquist plot of composite electrode

Conclusion

In a word, we successfully prepared a unique and uniform superstructure POAP/PPD-rGO. Simple operation and low cost are the advantage of the synthesis process. In the electrochemical test, the C_s of the composite electrode reached 1180 F/g at 1.0 A/g and the capacitance retention was approximately 91% after 3000 cycles. The reason this new electrode material showed good pseudo-capacitance performance was related to the following: First, the unique porous superstructure allowed for sufficient diffusion of the electrolyte and fast electron transfer. Second, the pore structure exposed a greater number of electrochemical active centers in the electrolyte. Third, in the amorphous state, the lattice energy of the material was low, and chemical intercalation/de-intercalation or redox reaction was facilitated.

Declarations

Conflict of interest The authors declare that they have no known competing financial interests or personal relationships that could have appeared to influence the work reported in this paper. There is no conflict of interest.

References

Bharath G, Veeramani V, Chen SM, Madhu R, Raja MM, Balamurugan A, Mangalaraj D, Viswanathan C, Ponpandian N (2015) Edge-carboxylated graphene anchoring magnetite hydroxyapatite nanocomposite for an efficient 4-nitrophenol sensor. RSC Adv 5:13392–13401

Burke A (2000) Ultracapacitors: why, how, and where is the technology. J Power Sources 91:37–50

Chen K, Xue D (2014) Preparation of colloidal graphene in quantity by electrochemical exfoliation. J Colloid Interface Sci 436:41–46

Chen K, Xue D (2015) In-situ electrochemical route to aerogel electrode materials of graphene and hexagonal CeO_2. J Colloid Interface Sci 446:77–83

Chen K, Xue D (2017) From graphite-clay composites to graphene electrode materials: In-situ electrochemical oxidation and functionalization. Mater Res Bull 96:281–285

Chen Z, Augustyn V, Wen J, Zhang Y, Shen M, Dunn B, Lu Y (2011) High performance supercapacitors based on intertwined CNT/V2O5 nanowire nanocomposites. Adv Mater 23:791–795

Chen K, Liu F, Xue D, Komarneni S (2015a) Carbon with ultrahigh capacitance when graphene paper meets K 3 Fe (CN) 6. Nanoscale 7(2):432–439

Chen K, Song S, Liu F, Xue D (2015b) Structural design of graphene for use in electrochemical energy storage devices. Chem Soc Rev 44(17):6230–6257

Chen K, Xue D, Komarneni S (2017) Nanoclay assisted electrochemical exfoliation of pencil core to high conductive graphene thin-film electrode. J Colloid Interface Sci 487:156–161

Dezfuli AS, Ganjali MR, Naderi HR, Norouzi P (2015) A high performance supercapacitor based on a ceria/graphene nanocomposite synthesized by a facile sonochemical method. RSC Adv 5:46050–46058

Drmosh QA, Yamani ZH, Hendi AH, Gondal MA, Moqbel RA, Saleh TA, Khan MY (2019) A novel approach to fabricating a ternary rGO/ZnO/Pt system for highperformance hydrogen sensor at low operating temperatures. Appl Surf Sci 464:610–626

Eftekhari A, Li L, Yang Y (2017) Polyaniline supercapacitors. J Power Sources 347:86–107

Ehsani A, Mahjani M, Jafarian M (2011) Electrochemical impedance spectroscopy study on intercalation and anomalous diffusion of $AlCl^-4$ ions into graphite in basic molten salt. Turk J Chem 35(5):735–743

Ehsani A, Mirtamizdoust B, Yousefi M, Safari R, Hadi M, Heidari AK (2018a) Nanocomposite of conjugated polymer/nano-flowers Cu (II) metal-organic system with 2-methylpyridinecarboxaldehyde isonicotinohydrazide as a novel and hybrid electrode material for highly capacitive pseudocapacitors. Bull Chem Soc Jpn 91:617–622

Ehsani A, Safari R, Yazdanpanah H, Kowsari E, Mohammad Shiri H (2018b) Electroactive conjugated polymer/magnetic functional reduced graphene oxide for highly capacitive pseudocapacitors: electrosynthesis, physioelectrochemical and DFT investigation. Electrochem Sci Technol 4:301–307

Ehsani A, Bigdeloo M, Lorparizangene A, Hadi M, Safari R, Mohammad Shiri H, Heidari AA (2019a) Carbon nanotube/metal oxide dispersed poly (ortho-aminophenol) as a ternary nanocomposite film: Facile electrosynthesis, surface characterization, and electrochemical pseudocapacitive performance. J Chin Chem Soc 66:396–401

Ehsani A, Parsimehr H, Nourmohammadi H, Safari R, Doostikhah S (2019b) Environment-friendly electrodes using biopolymer chitosan/poly ortho aminophenol with enhanced electrochemical behavior for use in energy storage devices. Polym Compos 40(12):4629–4637

Ehsani A, Bigdeloo M, Assefi F, Kiamehr M, Alizadeh R (2020) Ternary nanocomposite of conductive polymer/chitosan biopolymer/metal organic framework: Synthesis, characterization and electrochemical performance as effective electrode materials in pseudocapacitors. Inorg Chem Commun 115:107885

Ehsani A, Moftakhar M, karimi F (2021a) Lignin-derived carbon as a high efficient active material for enhancing pseudocapacitance performance of p-type conductive polymer. J Energy Storage 35:102291

Ehsani A, Mirtamizdoust B, karimi F, Bigdeloo M, Parsimehr H (2021b) Influence of nanostructured VO-acetylacetonate coordination system with 2-(pyridin-4-ylmethylene) hydrazine-1-carbothioamide in pseudocapacitance performance of p-type conductive polymer composite film. Plast Rubber Compos Macromol Eng 50(4):172–179

Ehsani A, Rezaei Z, Agah A, Mohammad Shiri H, Heidari AA (2021c) Electrochemical and theoretical investigation of functionalized reduced graphene aerogel modified electrode for lead ions sensing. Microchem J 165:106074

Ehsani A, Esfahaniha M, Khodaei kahriz P, Safari R, Parsimehr HR (2021d) Functionalized graphene oxide aerogel as a high efficient material for electrochemical sensing of organic pollutant. Surf Interface 22:100817

Gholipour-Ranjbar H, Ganjali MR, Norouzi P, Naderi HR (2016) Electrochemical investigation of functionalized graphene aerogel with different amount of p-phenylenediamine as an advanced electrode material for supercapacitors. Mater Res Express 3:075501

Hu L, Chen W, Xie X, Liu N, Yang Y, Wu H, Yao Y, Pasta M, Alshareef HN, Cui Y (2011) Symmetrical MnO2–carbon nanotube–textile nanostructures for wearable pseudocapacitors with high mass loading. ACS Nano 5:8904–8913

Kaempgen M, Chan CK, Ma J, Cui Y, Gruner G (2009) Printable thin filmsupercapacitors using single-walled carbon nanotubes. Nano Lett 9:1872–1876

Kahriz P, Mahdavi H, Ehsani A, Heidari A, Bigdeloo M (2020) Influence of synthesized functionalized reduced graphene oxide aerogel with 4,4′-methylenedianiline as reducing agent on electrochemical and pseudocapacitance performance of poly orthoaminophenol electroactive film. Electrochim Acta 354:136736

Kang Y, Zou D, Zhang J, Liang F, Hayashi K, Wang H, Sun X (2017) Dual–phase spinel MnCo2O4 nanocrystals with nitrogen-doped reduced graphene oxide as potential catalyst for hybrid Na–air batteries. Electrochim Acta 244:222–229

Kong F, Chen K, Song S, Xue D (2018) Metal organic framework derived CoFe@ N-doped carbon/reduced graphene sheets for enhanced oxygen evolution reaction. Inorganic Chem Front 5(8):1962–1966

Kumar V, Gupta RK, Gundampati RK, Singh DK, Mohan S, Hasan SH, Malviya M (2018) Enhanced electron transfer mediated detection of hydrogen peroxide using a silver nanoparticle–reduced graphene oxide–polyaniline fabricated electrochemical sensor. RSC Adv 8:619–631

Liu F, Xue D (2013) An electrochemical route to quantitative oxidation of graphene frameworks with controllable C/O ratios and added pseudocapacitances. Chem A Eur J 19(32):10716–10722

Liu F, Xue D (2015) Electrochemical energy storage applications of "pristine" graphene produced by non-oxidative routes. Sci China Technol Sci 58(11):1841–1850

Liu F, Song S, Xue D, Zhang H (2012) Folded structured graphene paper for high performance electrode materials. Adv Mater 24(8):1089–1094

Mahdavi H, Kahriz PK, Gholipour-Ranjbar H, Shahalizade T (2017) Synthesis and performance study of amino functionalized graphene aerogel grafted with polyaniline nanofibers as an efficient supercapacitor material. J Mater Sci: Mater Electron 28:4295–4305

Mahjani MG, Ehsani A, Jafarian M (2010) Electrochemical study on the semiconductor properties and fractal dimension of poly ortho aminophenol modified graphite electrode in contact with different aqueous electrolytes. Synth Met 160:1252–1258

Meng Y, Wang K, Zhang Y, Wei Z (2013a) Hierarchical porous graphene/polyaniline composite film with superior rate performance for flexible supercapacitors. Adv Mater 25:6985–6990

Meng Y, Wang K, Zhang Y, Wei Z (2013b) Hierarchical porous graphene/polyaniline composite film with superior rate performance for flexible supercapacitors. Adv Mater 25(48):6985–6990

Mohilner DM, Adams RN, Argersinger WJ (1962) Investigation of the kinetics and mechanism of the anodic oxidation of aniline in aqueous sulfuric acid solution at a platinum electrode. J Am Chem Soc 84:3618–3622

Moussa M, El-Kady MF, Zhao Z, Majewski P, Ma J (2016) Recent progress and performance evaluation for polyaniline/graphene nanocomposites as supercapacitor electrodes. Nanotechnology 27:442001

Naseri M, Fotouhi L, Ehsani A, Shiri H (2016) Novel electroactive nanocomposite of POAP for highly efficient energy storage and electrocatalyst: electrosynthesis and electrochemical performance. J Colloid Interface Sci 484:308–313

Peng H, Mo X, Liao S, Liang H, Yang L, Luo F, Song H, Zhong Y, Zhang B (2013) High performance Fe-and N-doped carbon catalyst with graphene structure for oxygen reduction. Sci Reports 3:1765

Sadeghi S, Mohammad Shiri H, Ehsani A, Oftadeh M (2020) Electrosynthesis of high-purity TbMn2O5 nanoparticles and its nanocomposite with conjugated polymer: surface, density of state and electrochemical investigation. Solid State Sci 105:106227

Sadeghinia M, Shabani Shayeh J, Fatemi F, Rahmandoust M, Ehsani A, Rezaei M (2019) Electrochemical study of perlite-barium ferrite/conductive polymer nano composite for super capacitor applications. Int J Hydrogen Energy 44:28088–28095

Shabani-Shayeh J, Ehsani A, Nikkar A, Norouzi P, Ganjali MR, Wojdyla M (2015) Physioelectrochemical investigation of the supercapacitive performance of a ternary nanocomposite by common electrochemical methods and fast Fourier transform voltammetry. New J Chem 39:9454

Shakir I, Almutairi Z, Shar SS, Nafady A (2020) Synthesis of $Co(OH)_2$/CNTs nanocomposite with superior rate capability and cyclic stability for energy storage applications. Mater Res Express 7:125501

Shayeh J, Sadeghinia M, Siadat S, Ehsani A, Rezaei M, Omidi M (2017) A novel route for electrosynthesis of $CuCr_2O_4$ nanocomposite with p-type conductive polymer as a high performance material for electrochemical supercapacitors. J Colloid Interface Sci 496:401–406

Shiri H, Ehsani A, Khales M (2017a) Electrochemical synthesis of Sm_2O_3 nanoparticles: application in conductive polymer composite films for supercapacitors. J Colloid Interface Sci 505:940–946

Shiri HM, Ehsani A, Khales MJ (2017b) Electrochemical synthesis of Sm_2O_3 nanoparticles: application in conductive polymer composite films for supercapacitors. J Colloid Interface 505:940–946

Shiri HM, Ehsani A, Behjatmanesh-Ardakani R (2018) Electrochemical deposition and plane-wave periodic DFT study on Dy_2O_3 nanoparticles and pseudocapacitance performance of Dy_2O_3/conductive polymer nanocomposite film. J Taiwan Inst Chem Eng 93:632–643

Shiri H, Ehsani A, Behjatmanesh-Ardakani R, Hajghani S (2019) Electrosynthesis of Y_2O_3 nanoparticles and its nanocomposite with POAP as high efficient electrode materials in energy storage device: surface, density of state and electrochemical investigation. Solid State Ionics 338:87–95

Yu C, Masarapu C, Rong J, Wei B, Jiang H (2009) Stretchable supercapacitors based on buckled single-walled carbon-nanotube macrofilms. Adv Mater 21:4793–4797

Yu H, Zhang B, Bulin C, Li R, Xing R (2016) High-efficient synthesis of graphene oxide based on improved hummers method. Sci Rep 6:36143

Zhang RHC, Liao H, Hou Y (2013) Synthesis of amino-functionalized graphene as metal-free catalyst and exploration of the roles of various nitrogen states in oxygen reduction reaction. Nano Energy 2:88–97

Zhao B, Liu P, Jiang Y, Pan D, Tao H, Song J, Fang T, Xu W (2012) Supercapacitor performances of thermally reduced graphene oxide. J Power Sources 198:423–427